



Contents lists available at SciVerse ScienceDirect

Mathematical and Computer Modelling

journal homepage: www.elsevier.com/locate/mcm

A green handover protocol in two-tier OFDMA macrocell–femtocell networks

Yuh-Shyan Chen*, Cheng-You Wu

Department of Computer Science and Information Engineering, National Taipei University, Taiwan, ROC

ARTICLE INFO

Article history:

Received 30 August 2011

Received in revised form 6 March 2012

Accepted 14 April 2012

Keywords:

Green handover

Energy-saving

Femtocell

OFDMA

Two-tier cellular networks

ABSTRACT

Femtocells are a promising technology to improve network performance with the short-range, low-power, and cost-beneficial small base stations. A femtocell is a low-power wireless access point that operates in licensed spectrum to connect a standard device to an operator's network using a digital subscriber line (DSL) connection. Most of the energy consumption of the telecommunication networks is caused by the base stations. It is important to reduce the energy consumption of the base stations for green ICT (information and communication technology). A two-tier orthogonal frequency-division multiple access (OFDMA) macro-femtocell network is a key issue to significantly reduce the total power consumption of the base stations. In this paper, we develop a green handover protocol in two-tier OFDMA macrocell–femtocell networks. The green handover protocol allows the femtocell base station to completely switch off its radio communication and associated processing when not involved in an active call. To improve the energy efficiency of femtocell base station, the proposed green handover protocol intelligently switches on its radio communication and associated processing, or called a “wake up” from the idle mode, if the remaining data of a mobile host can be completely uploaded through the wake-up femtocell base station. Finally, the mathematical analysis and the performance simulation illustrate that the proposed protocol provides a more power-saving result compared with existing energy-saving handover protocols.

© 2012 Elsevier Ltd. All rights reserved.

1. Introduction

Over 90% of the power in mobile communications is consumed in the radio access network [1]. For green communication, the power consumption of the radio access networks, including the base stations, must be reduced. Informa Telecoms & Media [2] expects the femtocell market to experience significant growth over the next few years, reaching just under 49 million femtocell access points (FAP) in the market by 2014 and 114 million mobile users accessing mobile networks through femtocells during that year. Assumed that each femtocell requires a power cost of 12 W, the total energy consumption of all deployed femtocells amount to 3.794×10^9 kWh/annum. Energy efficiency of femtocells becomes an urgent issue. In general, femtocells in active mode usually produce in the order of 2.05 million tones of CO₂ per year. To reduce the impact of information and communication technologies (ICTs) on environment, efforts for energy efficiency recently have received lots of attention, and a new concept has appeared – “Green Radio”, which means reducing the CO₂ emissions in ICTs. One useful way is to provide an energy efficient protocol to reduce the unnecessary power consumption of femtocells.

While the next-generation wireless technologies continue to evolve, mobile communications have also transformed from traditional voice services to IP-based services. LTE-advanced has been developed to redefine the traditional physical-layer

* Corresponding author. Tel.: +886 2 2748189 67072.

E-mail address: yschen@mail.ntpu.edu.tw (Y.-S. Chen).

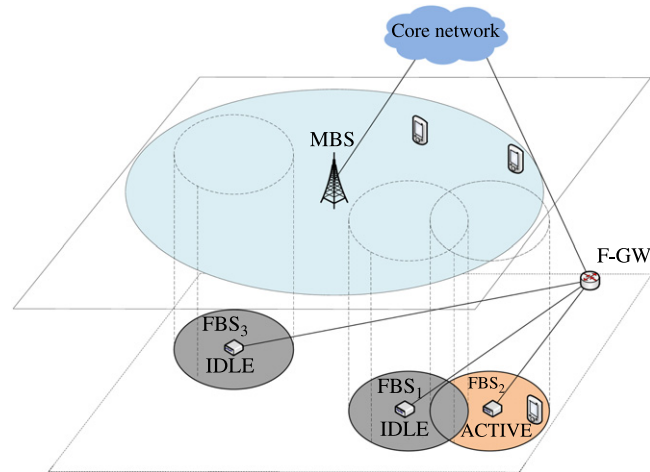


Fig. 1. Two-tier OFDMA macrocell-femtocell networks.

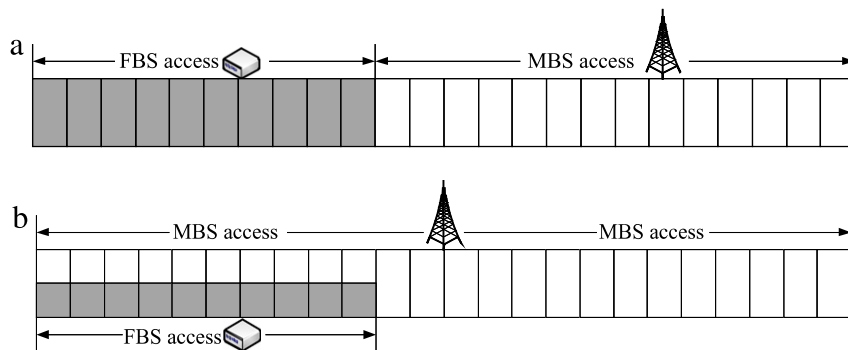


Fig. 2. Channel operation of two-tier networks. (a) Co-channel operation. (b) Dedicated channel operation.

air interface to produce a high transmission rate. With the emerging technology; such as Orthogonal Frequency Division Multiple Access (OFDMA) [3], LTE-advanced is expected to improve end-user throughputs and network capacity with the full mobility. In the LTE-advanced system, the total spectrum is partitioned into several pieces of spectrum which is denoted as “resource block (RB)” or “tile”. This work can be achieved with IP mobility support. Existing IP mobility works being achieved in the IETF are classified into “host-based mobility approach”, e.g., Mobile IPv6 and its extensions [4] and “network-based mobility approach” e.g., Proxy Mobile IPv6, [5–7].

A femtocell [8] is a low power, low cost, and user-deployed cellular base station (BSs) with a small coverage range (e.g. 30–40 m in diameter). A large number of femtocells are deployed in the coverage area of macrocells. The main purpose is to increase the indoor coverage for voice and high speed data services. A femtocell works on the licensed band and connects to the operator core network via DSL broadband backhaul. Fig. 1 shows a hierarchical radio access network which is a two-tier macrocell/femtocell network. The macrocell base station refers to eNB or MBS and the femtocell base station refers to HeNB or FBS in the two-tier cellular networks. In Fig. 1, the dark circle representing an FBS is in the IDLE mode and the light circle denotes an FBS is in the ACTIVE mode. All FBSs or HeNBs connect to the core network through FBS-GW (femto base station gateway).

There are three access control strategies in a femtocell; open, closed, and hybrid access modes. In the open access mode, all user equipments (UEs) can access any femtocells. In the closed access mode, any UE which is not member of the closed subscriber group (CSG) would not get access to the femtocell. In the hybrid access mode, part of the femtocell resources are operated in the open access, while the remaining femtocells follow the CSG access mode. The femtocell has two spectrum allocation modes; co-channel and dedicated channel modes [9], as shown in Fig. 2. In the dedicated channel mode, the free frequency bands are divided into two parts. One part of channels is solely used by the femtocells, and another part of channels is only used by the macrocell. The advantage of the dedicated channel mode is that the potential interference between macrocell and femtocells can be minimized. There will be low spectrum efficiency and reuse. In the co-channel mode, all free channels can be non-simultaneously shared by femtocells and macrocell. The spectrum efficiency of the co-channel channel mode is high. This paper assumes the co-channel channel mode for our protocol design.

In this paper, a new green handover protocol is designed in two-tier OFDMA macrocell-femtocell networks. The green handover protocol can intelligently switch on the radio communication and associated processing, or “wake up” from the

Table 1

Comparison of existing handover protocols for OFDMA two-tier macrocell–femtocell networks.

Category	No power saving schemes				Power saving schemes	
Property	Protocol					
	Moon protocol [12]	Wu protocol [13]	Ulvan protocol [14]	Zhang protocol [15]	Ashraf protocol [19]	The proposed protocol
Velocity of user	No	Yes	Yes	Yes	No	Yes
Signal strength	Yes	Yes	Yes	No	Yes	Yes
Traffic load	No	No	No	No	No	Yes

IDLE mode, of a femtocell. The smart decision of the “wake up” operation is based on the fact that the remaining data of a mobile host can be completely uploaded through the wake-up FBS.

The rest of this paper is organized as follows. Section 2 describes the related works and motivation. In Section 3, the system model, problem formulation, and basic idea are described. Section 4 describes the proposed green handover protocol in OFDMA two-tier macrocell–femtocell networks. Simulation results are presented in Section 5. Section 6 concludes this paper.

2. Related work

This section describes related works and motivation in Section 2.1 and the problem formulation in Section 2.2.

2.1. Related work

The deployment of femtocells benefits both users and service providers. Subscribers accessing femtocells can achieve greater signal strength and better quality of service because of the short transmit–receive distance. The mobility managements [10–12], need to be carefully addressed and investigated.

Existing results of the mobility management had been widely developed in OFDMA two-tier macrocell–femtocell networks [13–16]. Table 1 gives four handover protocols without the power saving consideration [13–16] and two handover protocols [17,18], including our developed protocol, with the power saving consideration. First, Moon and Cho [13] introduced an RSS-based handover decision protocol in hierarchical macro/femto-cell networks. The main idea is to combine the value of the received signal strength from a serving MBS and a target FBS with the consideration of the large asymmetry in their transmit powers. Not only considering the SNR, some other results further consider the UE speed for handover protocol designs [14–16]. Wu et al. [14] proposed a handover algorithm in the two-hierarchy network by considering both signal strength and velocity. Ulvan et al. [15] and Zhang et al. [16] recently proposed new handover algorithms in LTE-based femtocell networks based on the speed of UE and Quality of Service (QoS). Three different velocity environments have been considered in the algorithms, i.e. low mobile state (0–15 km/h), medium mobile state (15–30 km/h) and high mobile state (> 30 km/h). In addition, the real-time and non-real-time traffics have been considered as QoS parameters. The main purpose of above mentioned algorithms is to achieve the seamless handover and reduce the handover latency. These algorithms consider signal-to-noise ratio (SNR) and velocity for designing the handover protocol, the power consumption of femtocell is not taken into account. However, these mobility protocols are not the power-saving solutions.

Cell power consumption issues are recently raised more attentions [19,17,18]. The 3GPP TS 36.927 (release 10) [19] defines potential solutions for energy saving for E-UTRAN, which indicates that the cell can be totally switched off during the energy saving (ES) procedure. The ES procedure may be triggered in case of the light traffic or no traffic. Since there are thousands of femtocells within a macrocell area, the femtocell deployments may increase energy consumption except for the case of low femtocell/user densities and the use of femtocells with “idle” mode. Ashraf et al. [17,18] recently proposed an improving energy efficiency of femtocell base station via user activity detection. The proposed energy-saving procedure allows the femto BS to completely switch off its radio transmissions and associated processing when not involved in an active call. From our point of view, this method is not really power-efficient of the femtocell power consumption. This is because that when the signal power of a UE is just bigger than a threshold value if the UE approaches to the coverage of femtocell, the femto base station is waked up to performs the handover procedure. It may causes the femtocell frequently switches between “wake up” and “sleep”. In addition, a dense two-tier macrocell–femtocell network is considered, implies that thousands of femtocell is deployed within a fixed macrocell area. In such scenario, the pilot signal of femtocell can radiate outside the premises, and hence provide undesired external coverage, moving UEs face up to the continual handovers when they pass along buildings. A frequent handover of UE suffers the increased signaling cost and low system performance. Therefore, it is important to design a new green handover by avoiding the undesired handover to reduce the unnecessary power consumption.

2.2. Motivation

The motivation of this work is stated as follows. Fig. 3 illustrates a drawback of Ashraf protocol [17,18]. Ashraf et al. [17,18] provided a dynamic energy-efficient solution to the power consumption of femtocell. However, it may possibly

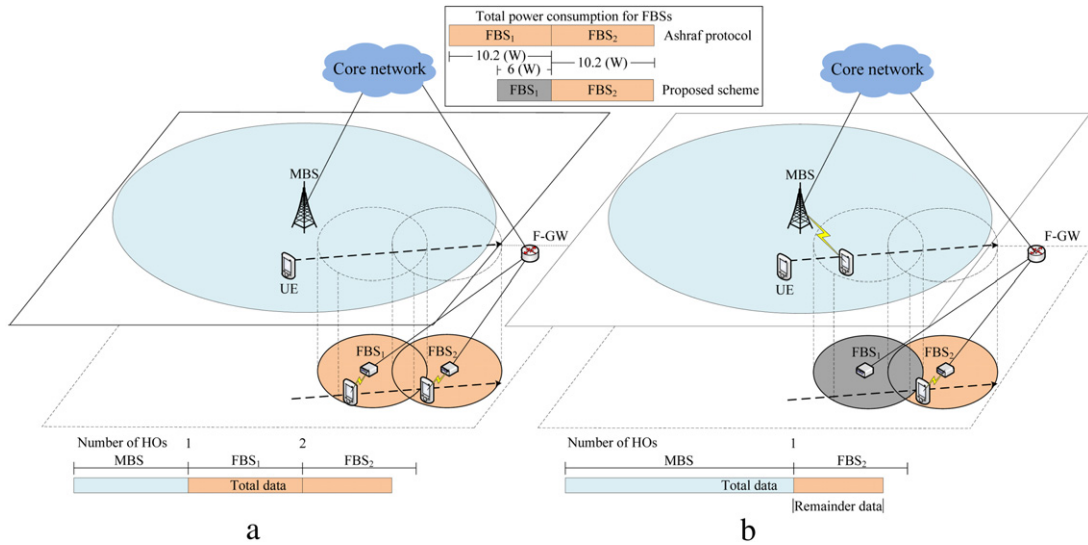


Fig. 3. Comparison of the power consumption and the number of handovers. (a) Ashraf protocol. (b) Our proposed protocol.

Table 2
Power consumption of femtocell and UE.

	Active	Idle	Power saving
Femtocell	10.2 (W)	6 (W)	4.2 (W)
	Connect to macrocell	Connect to femtocell	Power saving
LTE UE	0.2 (W)	0.0001 m (W)	≈ 0.2 (W)
GSM UE	2 (W)	3.2 (W)	1.9968 (W)

produce an undesired handover problem as follows. A FBS must be wake up from the “idle” state, only if the received signal strength of a moving UE from the FBS exceeds a predetermined threshold. We observed that if a moving UE cannot completely transmit all of the remainder data through the “wake-up” FBS, then the total power consumption may be higher than that of the FBS under the FBS is not “wake up”. For the more power-saving purpose, efforts will be done to intelligently make the decision of wake-up and handover.

Table 2 provides the fact that the power consumption of data transmission between femtocell and UE [17,18]. The LTE UE and GSM UE connecting to macrocell spend about 0.2 and 2 W, but LTE UE and GSM UE connecting to femtocell spend about 0.0001 and 3.2 mW. The extra power consumption of LTE UE and GSM UE are about 0.2 and 1.9968 W if UE is adopted the MBS for the data transmission. The femtocell operating in the ACTIVE mode spends 10.2 W and operating in the IDLE mode spends 4.2 W. If LTE UE communicates with macrocell and femtocell keeps the IDLE mode, then the power-saving is equal to $4.2 \text{ W} = 10.2 - 6 \text{ W}$. In such situation, it is more power-saving since $4.2 \text{ W} > 0.2$ and 1.9968 W . That is to say, if we try to keep the femtocell at the IDLE mode as possible, the more power-saving will be.

To overcome the mentioned drawback, a new green handover procedure is developed to minimize the power consumption of FBS and the handover cost. The objective of the paper is; (1) the overall system power consumption of the two-tier macrocell–femtocell network, is minimized by intelligently switching on/off its radio communication and associated processing, which aims to keep the femtocell at the IDLE mode as far as possible, (2) a handover decision protocol is designed to reduce the handover number and the signaling cost during the UE mobility.

3. Preliminaries

This section describes the system model, problem formulation, and basic idea in Sections 3.1–3.3.

3.1. System model

The system model of a two-tier OFDMA macrocell–femtocell network is illustrated in Fig. 4. A large number of femtocells are deployed in the coverage area of macrocells. Let MBS_i denote any one of macro base stations, where $1 \leq i \leq M$, and M is the maximum number of macro base stations of the coverage area of macrocells. Given MBS_i , let FBS_j denote as one femto base station, where $1 \leq j \leq N$, where N is the total number of femtocells within the coverage area of MBS_i . Both MBS_i and FBS_j adopt OFDMA technology under the co-channel model [9] to share all spectrum bands. The MBS_i connects

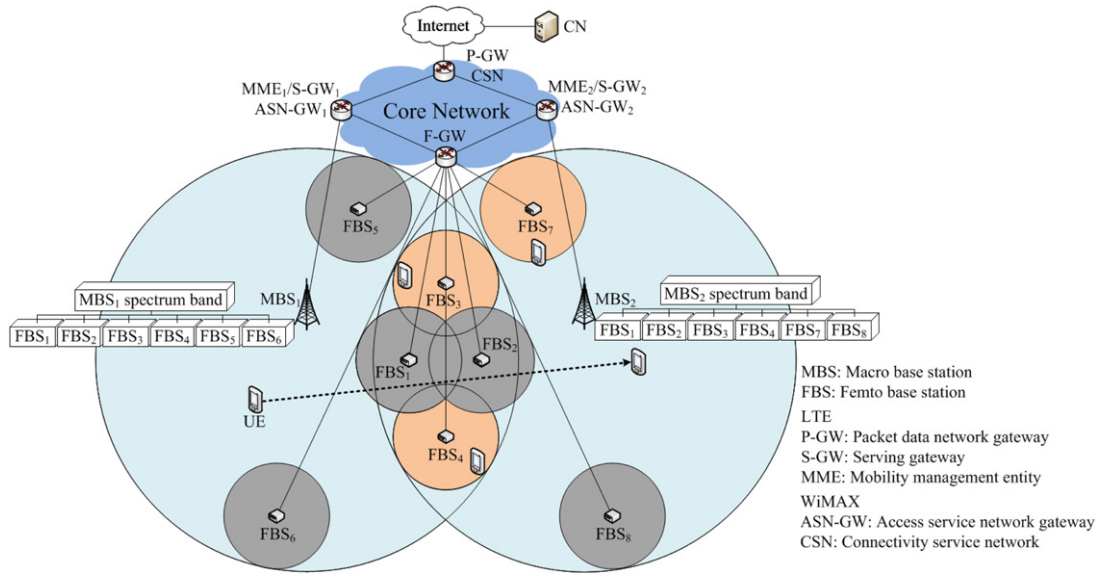


Fig. 4. The two-tier OFDMA macrocell-femtocell networks architecture.

to the core network through $MME_i/S-GW_i$ (Mobility Management Entity/Serving Gateway) or ASN/GW_i (Access Service Network/Gateway) for LTE/LTE-advanced or WiMAX networks. The FBS_j connects to core node through F-GW (femtocell-Gateway).

For example as shown in Fig. 4, FBS_5 and FBS_6 share the spectrum bands of MBS_1 , and FBS_7 and FBS_8 share the spectrum bands of MBS_2 . In addition, FBS_1 , FBS_2 , FBS_3 , and FBS_4 , are deployed in the overlap area of MBS_1 and MBS_2 . Dark and light circles denote the IDLE FBS and ACTIVE FBS, where an FBS is called an IDLE FBS if the FBS is in the IDLE mode, and a FBS is called an ACTIVE FBS if the FBS is in the ACTIVE mode. Each FBS has a small signal coverage (e.g. 30–40 m in diameter) determined by the maximum transmit power of the base station. An ACTIVE FBS may have multiple connected UEs. We follow the model of [17,18]. An IDLE FBS allows the FBS to switch off all pilot transmissions and the processing associated with the wireless reception, when no user is involved in an active call. Due to the two-tier macrocell-femtocell network model considered, the underlay macrocell coverage is required for enabling the IDLE mode procedure since it relies on detecting transmission from a UE to a macrocell. If there is an idle UE within an FBS in the two-tier macrocell-femtocell network, the synchronization of idle UEs is still guaranteed by the macro BS.

Fig. 5 illustrates the power consumption of hardware modules of IDLE FBS and ACTIVE FBS. We follow the same model of [17,18]. All of the hardware modules are divided into three parts. The first part is random access memory components connected to the microprocessor required for data handling functions. The second part is a field-programmable gate array (FPGA) and integrated circuitry to implement the data encryption, the hardware authentication, and the network time protocol. The third part is the RF transceiver, including separate RF components for the packet transmission and reception. A RF power amplifier (PA) is also needed to pass a high-power signal to the transmitting antenna. Fig. 5(a) shows the power consumption for all components of ACTIVE FBS and Fig. 5(b) shows the power consumption of IDLE FBS. The two modes are only different in the power consumption of all modules. When switching to IDLE mode, a FBS switches off the PA, RF transmitter, RF receiver, and miscellaneous hardware components related to non-essential functionalities, such as data encryption, hardware authentication. Following the power consumption of the chipset [19,20], a radio sniffer ($P_{sniffer} = 0.3$ W) function is switched on to received power measurement of MBS and UE. The power consumption of an ACTIVE FBS is about 10.2 W. The power consumption of an IDLE FBS is 6 W. When an FBS switches from ACTIVE to IDLE mode, the power saving is about 4.5 W.

3.2. Problem formulation

The problem of designing a green handover protocol in two-tier OFDMA macrocell-femtocell networks is formally described as follows: (1) A UE is moving from MBS_i to MBS_{i+1} , the UE passes through many FBSs. Assuming that the UE enters the coverage of an IDLE FBS_j , the UE detects the pilot power of the IDLE FBS_j is larger than that of the serving MBS_i , a smart handover procedure is initiated to make a decision to wake up the FBS_j from IDLE to ACTIVE modes or not, to avoid the undesired “wake up” and handover process. (2) The heavy handover signaling costs cause a system burden due to the occurring the undesired handovers. This problem is considered in our protocol. (3) The total power consumption is high if IDLE FBS_j makes the wrong decision of “wake up” and handover. This smart decision is based on estimated values of t_{dwell} and $t_{expected}$, where t_{dwell} is the dwell time of a UE of keeping the communication with FBS_j , where the UE is in the coverage

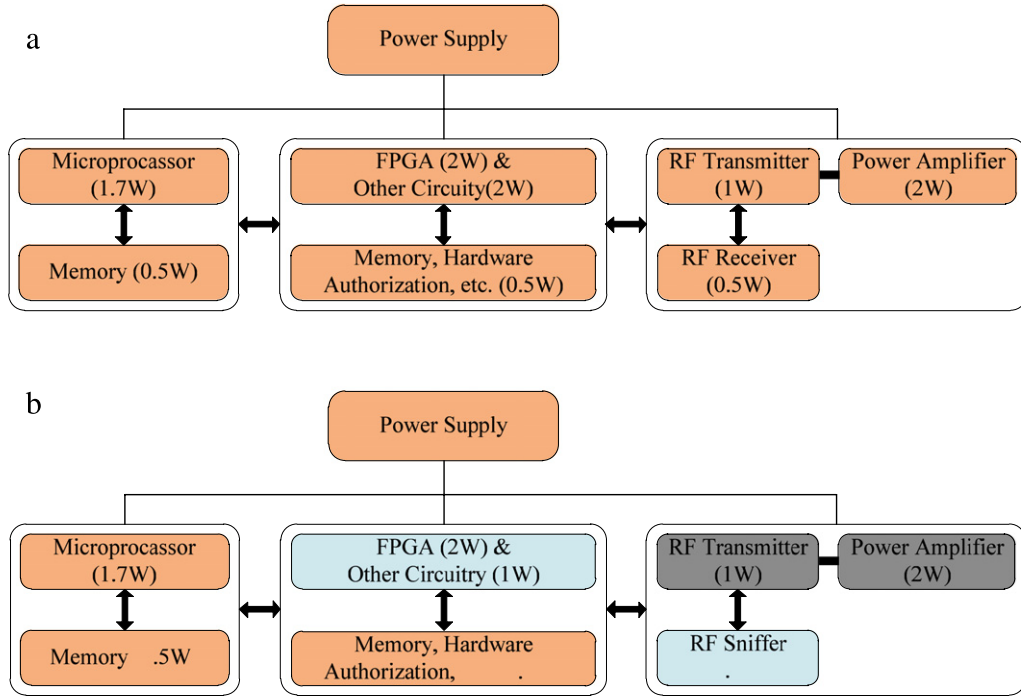


Fig. 5. Power consumption of the femtocell hardware. (a) ACTIVE mode. (b) IDLE mode.

of FBS_j and t_{expected} is the expected transmission time of data of the UE. If a UE cannot completely transmit all of the data within the t_{dwell} , then an IDLE FBS_j should not become ACTIVE FBS_j and cannot handover from MBS_i to FBS_j .

3.3. Basic idea

Before describing the basic idea, some notations are defined as follows. As mentioned before, an energy-saving handover is developed based on the estimated values of t_{dwell} and t_{expected} .

Definition 1 (t_{dwell} Dwell Time). Given a UE and an FBS, let t_{dwell} denote the time period from the UE starting to communicate with the FBS to the UE stopping to communicate with the FBS, where the UE is in the coverage of the FBS. The UE may communicate with a corresponding node (CN) through the FBS, within the t_{dwell} .

Definition 2 (t_{expected} Average Expected Transmission Time). Let t_{expected} denote the expected transmission time between the UE and the FBS, where t_{expected} is equal to the remainder data of the UE divided by the average transmission rate between the UE and the FBS, within t_{dwell} .

Definition 3 (Green Handover). A handover is called a green handover if the handover is an energy-saving handover with minimized power consumptions of base station and the UE during the handover period. The base station switches off its hardware modules for the power-saving if no active user is resident in the coverage of the base station.

The basic idea of the green handover is to keep the FBS at the IDLE mode as far as possible. To achieve the purpose, t_{dwell} and t_{expected} are needed to be calculated as illustrated in Fig. 6. It is observed that an FBS switches from IDLE mode to ACTIVE mode only if $t_{\text{expected}} < t_{\text{dwell}}$. But if $t_{\text{expected}} \geq t_{\text{dwell}}$, then the FBS should not be woken up from the IDLE mode, and the UE still connects with the MBS and does not perform the handover procedure.

To state the basic idea of our protocol, and the key difference of our protocol with the Ashraf protocol [17,18] are compared in Fig. 3. Fig. 3(a) illustrates the Ashraf protocol [17,18] by introducing the IDLE mode to the normal femtocell operation to disable the pilot transmissions and the associated radio processing if there is no active call. When a UE located inside the coverage range of the FBS, and the UE already makes a call to the MBS, FBS sniffs a rise in the received power on the uplink frequency band. If the received signal strength from UE of a FBS exceeds a predetermined threshold, then a wake-up and handover operation of the FBS are performed. By experience, it is difficult to determine the optimal threshold value.

Fig. 3(b) illustrates the basic idea of our proposed scheme by an example. When a UE moves from left to right, the UE passes through two FBSs; FBS_1 and FBS_2 . When the UE enters the coverage of FBS_1 , the uplink signal power of the UE is

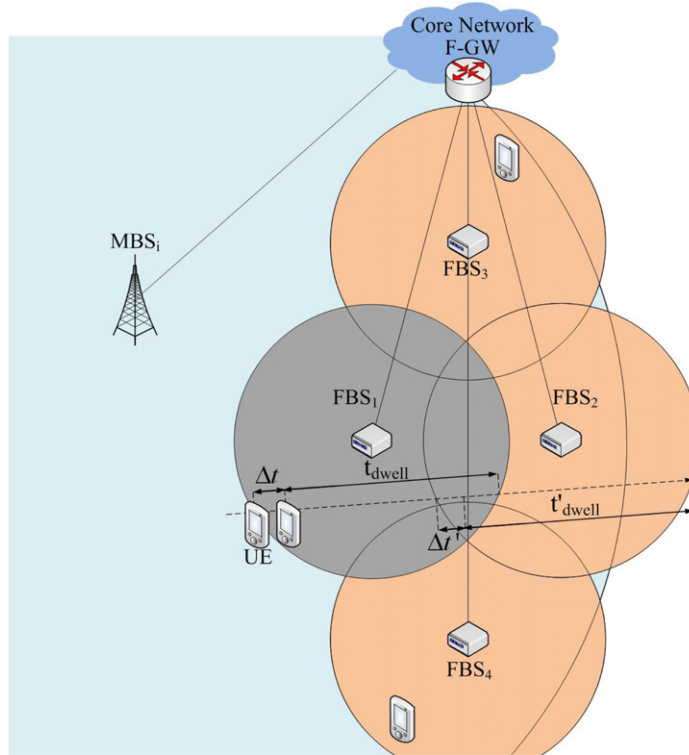


Fig. 6. The dwell time and the average expected transmission time.

received by FBS_1 . The FBS_1 constructs the free spectrum bands, denoted as $I_{available}^{FBS_1}$, by sending a request to/from neighbor FBSs and the serving MBS. The FBS_1 calculates times of t_{dwell} and $t_{expected}$ to estimate the required bandwidth which can completely transmit the reminder data through FBS_1 within the t_{dwell} , which is denoted as $I_{request}^{UE}$. If $I_{available}^{FBS_1} \geq I_{request}^{UE}$, FBS_1 is wake-up to prepare to perform the handover operation from serving MBS to FBS_1 . If $I_{available}^{FBS_1} < I_{request}^{UE}$, then the FBS_1 is not wake-up, and the UE still transmit the reminder data through the serving MBS. Our scheme provides a more accurately wake-up decision scheme to reduce the times of unnecessary wake-up and handover operations to reduce the total power consumptions. It is observed that if the UE continually enters the coverage of FBS_2 , then FBS_1 must re-enter the IDLE mode. It surely takes more power consumption to wake up the FBS_1 and perform the handover operation from MBS to FBS_1 if the data transmission cannot be completely done through FBS_1 . The aims of this work is to provide an accurately wake-up decision scheme to reduce the times of un-necessary wake-up and handover operations to reduce the total power consumptions.

The main contribution of this paper is to achieve energy saving for the overall radio access network by keeping the femtocell in the IDLE mode as far as possible. In the two-tier OFDMA macrocell-femtocell network, a large number of FBSs are deployed in the MBS networks but some FBSs are not needed to be switched on. The total number of handovers and the power consumption can be significantly reduced if we intelligently keep possible FBSs in the IDLE mode. The main work is to develop a new green handover protocol to intelligently keep FBSs in the IDLE mode to significantly improve the total number of handovers and the power consumption.

4. A green handover protocol

We first give an overview of our green handover protocol in OFDMA two-tier macrocell-femtocell networks. The main function of the green handover protocol is to make an intelligent decision of accurately wake-up the FBS from IDLE mode into ACTIVE mode at the right time and at the right place. This is mainly based on the prediction of the dwell time t_{dwell} and average expected transmission time $t_{expected}$ of the UE. The detailed flow chart of the green handover protocol is firstly shown in Fig. 7. The developed protocol consists of three phases: free spectrum configuration, transmission time estimation, and green handover decision phases, which are described below.

1. *Free spectrum configuration phase*: This phase is to identify a configuration of the free spectrum band for a FBS_j , assumed that the FBS_j is considered to be switched from IDLE mode into ACTIVE mode, and FBS_j is located at the overlapped area between MBS_i and MBS_{i+1} , where MBS_i is serving MBS and MBS_{i+1} is the next MBS. By using the co-channel channel mode [9], the FBS_j can access all free spectrum bands of MBS_i or MBS_{i+1} , but cannot simultaneously use the same frequency band due to avoiding the interference problem. In addition, the FBS_j also cannot simultaneously use the same frequency

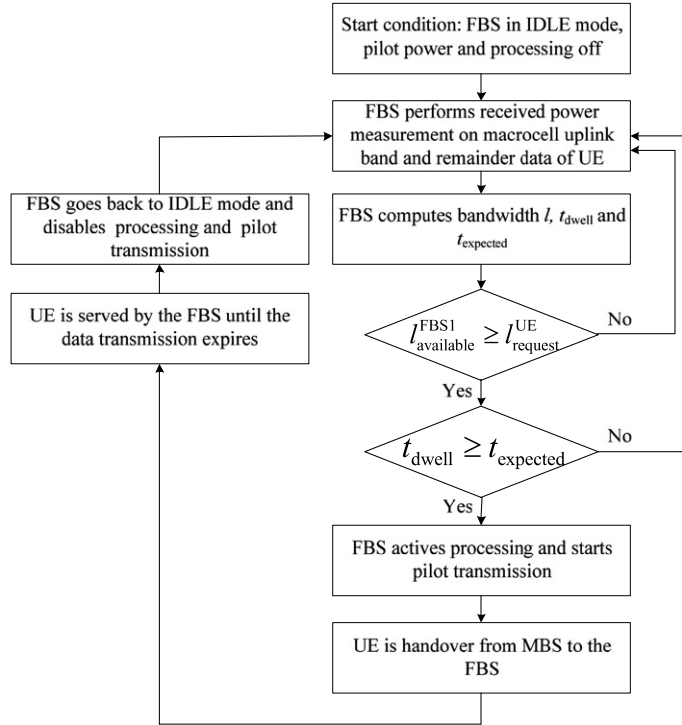


Fig. 7. The flow chart of the green handover protocol.

band of all neighboring FBS_j . This phase identifies the free and useful spectrum bands by excluding all used spectrum bands of MBS_i (or MBS_{i+1}), and all neighboring FBS_j . It is observed that our work also can be successfully applied when the FBS_j is not located at the overlapping area between MBS_i and MBS_{i+1} . By the co-channel channel mode [9], all the spectrum bands of MBS_i and MBS_{i+1} are different, therefore we just need to consider to avoid the used spectrum bands of MBS_i or MBS_{i+1} .

2. *Transmission time estimation* phase: The task of the phase is to calculate the dwell time t_{dwell} and average expected transmission time $t_{expected}$ by FBS_j before the UE performing a wake-up decision and a handover procedure from MBS_i to FBS_j .
3. *Green Handover decision* phase: The phase makes a wake-up and handover decision based on the dwell time t_{dwell} and average expected transmission time $t_{expected}$. The simple concept for the green handover decision is checked if the remainder data of UE can completely transmitted by (i.e., $t_{expected} \leq t_{dwell}$), then FBS_j should be woken up from the IDLE mode and enters the ACTIVE mode to perform the handover procedure for the inbound mobility (mobility from macrocell to femtocell).

The detailed operations of the free spectrum configuration, transmission time estimation, and the green handover decision phases are described as follows.

4.1. Phase I: Free spectrum configuration

This paper inherits existing resource sharing results from [21–23], which is stated as follows. Initially, the FBS choses the spectrum band of a MBS under the co-channel model. The MBS allocates its spectrum resources to MBS UEs and FBSs, and then the FBS re-allocates its allocated spectrum resources to FBS UEs. The spectrum band means the available bandwidth which can be accessed by UEs. The FBS_j cannot simultaneously connect to another FBS GW and another MME. This phase is to identify the free spectrum for IDLE FBS_j . Let G denote the set of spectrum sharing groups, let MBS_i , $1 \leq i \leq m$ denote the i -th MBS, let $FBS_j^{i'}$, $1 \leq i' \leq n$ denote the neighboring FBSs of j -th FBS.

Let $S_{MBS_i} = \{T_1, T_2, \dots, T_\beta\}$ denote the set of the original unused spectrum bands of MBS_i , and let $SB_{MBS_i} = \{o_1, o_2, \dots, o_i, \dots, o_z \mid o_i \in S_{MBS_i}, z \leq \beta\}$ denote the set of occupied sub-bands by MBS_i , $1 \leq i \leq m$. Let $SB_{FBS_j^{i'}} = \{o_1^{i'}, o_2^{i'}, \dots, o_i^{i'}, \dots, o_{z'}^{i'} \mid o_i^{i'} \in S_{MBS_i}, z' \leq \beta\}$ denote the set of occupied sub-bands by $FBS_j^{i'}$, $1 \leq i' \leq n$. As mentioned before, $I_{available}^{FBS_j}$ is denoted as the free spectrum bands of FBS_j . The detailed steps of the free spectrum configuration are described as follows.

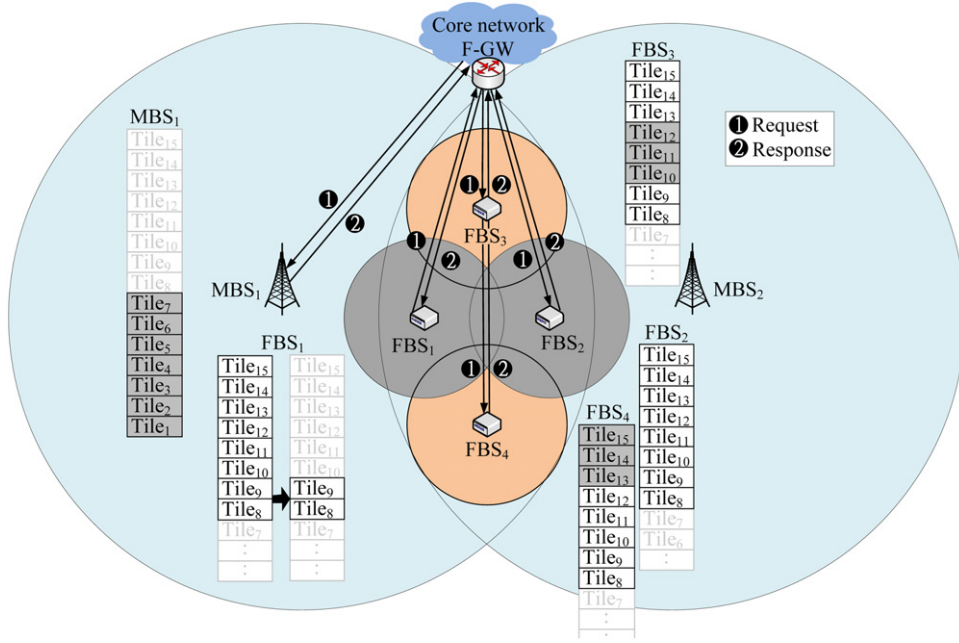


Fig. 8. The free spectrum configuration.

1. Given a UE, considered the serving MBS_i and IDLE FBS_j , and all neighboring FBSs of FBS_j , $FBS_{j'}^i$, $1 \leq i' \leq m$.
2. When the UE enters into the coverage of FBS_j , the FBS_j requests the information of $SB_{MBS_i} = \{o_1, o_2, \dots, o_i, \dots, o_z \mid o_i \in S_{MBS_i}, z \leq \beta\}$ from MBS_i via F-GW. In addition, the FBS_j requests the information of $SB_{FBS_{j'}^i} = \{o_{i'}^j, o_{i'}^j, \dots, o_{i'}^j, \dots, o_{z'}^j \mid o_{i'}^j \in S_{MBS_i}, z' \leq \beta\}$ from all neighboring FBSs of FBS_j via the backhaul network.
3. Let $S_{occupied}$ denote as the union of occupied spectrum bands of MBS_i and all occupied spectrum bands of $FBS_{j'}^i$, for $1 \leq i' \leq n$. Therefore, $S_{occupied} = SB_{MBS_i} \cup \left(\bigcup_{i'=1}^n SB_{FBS_{j'}^i} \right)$. Then $l_{available}^{FBS_j} = S_{MBS_i} - S_{occupied}$.

Fig. 8 shows an example of the free spectrum configuration, the total spectrum resource of S_{MBS_1} is $\{T_1, T_2, \dots, T_{15}\}$ and $SB_{MBS_1} = \{T_1, T_2, \dots, T_7\}$. Let FBS_1 and FBS_2 be in IDLE mode and FBS_3 and FBS_4 be in ACTIVE mode. The neighboring FBSs of FBS_1 are $FBS_1^2 = FBS_2$, $FBS_1^3 = FBS_3$, and $FBS_1^4 = FBS_4$. A UE tries to perform the inbound mobility operation from MBS_1 to FBS_1 . Initially, we have $SB_{MBS_1} = \{T_1, T_2, \dots, T_7\}$, $SB_{FBS_2} = \{T_8, T_9, \dots, T_{15}\}$, $SB_{FBS_3} = \{T_{10}, T_{11}, T_{12}\}$, and $SB_{FBS_4} = \{T_{13}, T_{14}, T_{15}\}$. Observe that, $SB_{FBS_2} = \{T_8, T_9, \dots, T_{15}\}$ because FBS_2 is operating in the IDLE mode. The total occupied spectrum band is $S_{occupied} = \{T_1, T_2, \dots, T_7, T_{10}, \dots, T_{15}\}$, then $l_{available}^{FBS_1} = S - S_{occupied}$, so $SB_{FBS_1} = \{T_8, T_9\}$.

4.2. Phase II: Transmission time estimation

This phase calculates the dwell time t_{dwell} , the average expected transmission time $t_{expected}$, and $l_{required}^{UE}$ for a UE trying to perform the inbound mobility from MBS_i to FBS_j , where $l_{required}^{UE}$ denotes the bandwidth of the UE required to completely upload reminder data within the dwell time t_{dwell} . This phase is also a positioning problem to estimate if a moving UE can completely upload the remaining data within the dwell time t_{dwell} or not.

Initially, the dwell time t_{dwell} is calculated as follows. The dwell time is the time period from when a UE starts to communicate with FBS_j to the UE leaving the FBS_j . Let SNR_{UE-FBS_j} denote the signal power between the UE and FBS_j . Let SNR_{UE-MBS_i} denote the signal power between the UE and MBS_i and let $SNR_{MBS_i-FBS_j}$ denote the signal power between MBS_i and FBS_j . This work assumes to avoid the effect of fast fading and shadowing. The path loss model is considered. Some existing avoiding of fast fading and shadowing can be additionally adopted to enhance the accuracy of estimating t_{dwell} . The procedure of calculating t_{dwell} is given as follows.

1. If a UE enters the coverage of the FBS_j at time t_i , there are three values of signal power, SNR_{UE-FBS_j} , SNR_{UE-MBS_i} , and $SNR_{MBS_i-FBS_j}$, can be received at FBS_j . With three values of signal power, the distances between UE and FBS_j (denoted as d_{U-F_j}), between UE and MBS_i (denoted as d_{U-M_i}), and between MBS_i and FBS_j (denoted as $d_{M_i-F_j}$) can be obtained. The values of SNR_{UE-FBS_j} and can be directly obtained by FBS_j . The value of SNR_{UE-MBS_i} is obtained from MBS_i to FBS_j through via the backhaul network.

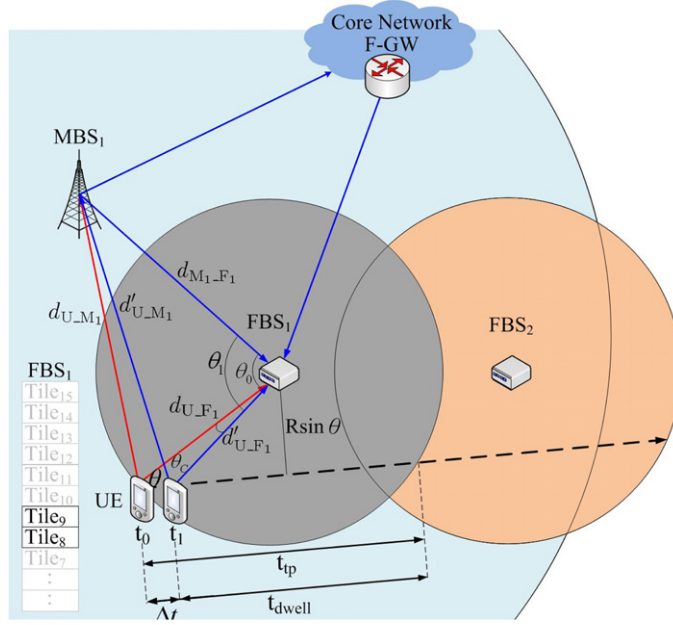


Fig. 9. The computation of the dwell time.

2. If the UE continually moves along the moving direction by the fixed speed, we may similarly obtain three distance values of d'_{U-F_j} , d'_{U-M_j} , and $d'_{M_i-F_j}$ at time t_{i+1} .
3. An angle θ_i between $d_{M_i-F_j}$ and d_{U-F_j} at time t_i and an angle θ_{i+1} between $d'_{M_i-F_j}$ and d'_{U-F_j} at time t_{i+1} can be calculated. An angle θ_C is equal to θ_{i+1} minus θ_i between d_{U-F_j} and d'_{U-F_j} . With the angle θ_C , an angle θ between d_{U-F_j} and the moving direction of the UE can be determined.
4. Let the expected maximum signal power of the UE at time t_{i+1} be denoted as SNR_{MAX} . We first consider the effect of the path loss. The path loss model [24] is adopted, such that $PL(d) = 38.46 + 20 \log_{10}(d) + 0.7d_{2D}$, where d is the distance of the UE and FBS_j , and $0.7d_{2D}$ is the penetration loss due to internal walls. In the case, $R \sin \theta$ is the shortest distance between UE and FBS_j thus the signal power becomes $SNR_{PL} = SNR_{UE} - PL(R \sin \theta)$, where SNR_{UE} is the original SNR of the UE at time t_{i+1} . Further, the effects of the fast fading and shadowing are considered, the expected maximum received signal strength can be represented as $SNR_{MAX} \frac{1}{\sqrt{2\pi\sigma_{dB}^2}} \exp \left[-\frac{(SNR_{PL} - \mu)^2}{2\sigma_{dB}^2} \right]$, from [25], where σ_{dB} is the standard deviation of shadowing and μ is the average power.
5. The t_{dwell} is predicted as follows. A passing time, denoted as t_{tp} , from the UE entering the coverage of the FBS_j to leaving the coverage of the FBS_j , is accurately calculated as follows. Let $\alpha = \frac{\int_R SNR_{MAX}}{\Delta t}$ denote as the average variation of SNR at Δt , where R and r are the distances between UE and FBS_j at times t_i and t_{i+1} and $\Delta t = t_{i+1} - t_i$, respectively. The half of t_{tp} is $\frac{SNR_{MAX}}{\alpha}$, so $t_{tp} = 2 \times \frac{SNR_{MAX}}{\alpha}$. Finally, the t_{dwell} is equal to $t_{tp} - \Delta t = t_{tp} - (t_{i+1} - t_i)$.

For example as illustrated in Fig. 9, the dwell time starts from time t_1 until the UE leaving the coverage of FBS_1 . A UE is moving and keeping the communication with MBS_1 in the coverage of FBS_1 . The FBS_1 receives SNR_{UE, FBS_1} , SNR_{UE, MBS_1} , and SNR_{MBS_1, FBS_1} at t_0 and t_1 . A first triangle is composed of d_{U-F_1} , d_{U-M_1} and $d_{M_1-F_1}$ at time t_0 . The angle $\theta_0 = \cos^{-1} \frac{d_{M_1-F_1}^2 + d_{U-F_1}^2 - d_{U-M_1}^2}{2d_{M_1-F_1}d_{U-F_1}}$. The second triangle is composed of d'_{U-F_1} , d'_{U-M_1} and $d'_{M_1-F_1}$ at time t_1 . Therefore, angle $\theta_1 = \cos^{-1} \frac{d_{M_1-F_1}^2 + d_{U-F_1}^2 - d_{U-M_1}^2}{2d_{M_1-F_1}d_{U-F_1}}$. Then, $\theta_C = \theta_1 - \theta_0$. We may have $d_{t_0-t_1} = \sqrt{d_{U-F_1}^2 + d_{U-F_1}^2 - 2d_{U-F_1}d'_{U-F_1} \cos \theta_C}$. Then, $\theta = \cos^{-1} \frac{d_{U-F_1}^2 + d_{U-F_1}^2 - d_{t_0-t_1}^2}{2d_{U-F_1}d'_{U-F_1}}$ is obtained. The variation of SNR per unit time, $\alpha = \frac{\int_{d_{U-F_1}}^{d'_{U-F_1}} SNR_{UE} - (38.46 + 20 \log_{10}(d) + 0.7d_{2D})d(d)}{t_1 - t_0}$. Therefore, $t_{tp} = 2 \times \frac{SNR_{MAX}}{\alpha}$ and $t_{dwell} = t_{tp} - (t_1 - t_0)$.

Second, the $I_{required}^{UE}$ is needed to be calculated as follows. We revise the result of the radio resource management from [20] to provide the probability of the packet delay and the probability of infraction used in this work. Let l denote as a tile number. Let n denote as the bit number of a tile (n bits). Let δ denote as an effective bandwidth determined by the arrival process and the service process. The procedure of calculating $I_{required}^{UE}$ is given as follows.

1. Considered a UE, an IDLE FBS_j initially allocates $l(=1)$ tile for the UE. Let $E_B^{UE}(\phi)$ [20] denote the effective bandwidth of the UE which specifies the maximum constant service rate required by a given arrival process subject to a given ϕ , where the ϕ is the indicator of QoS guarantees that can be provided by the FBS_j . Let $E_C^{(UE,1)}(\phi)$ denote the effective capacity of the UE which is allocated by l tiles. Find the solution of ϕ such that $E_B^{UE}(\phi) = E_C^{(UE,1)}(\phi) = \delta$ where the effective capacity $E_C^{(UE,1)}(\phi) = \frac{1}{\phi} \log(e^{-n\phi})$ [20]. Go to step 3.
2. Based on the result of [20], if $l \neq 1$, the effective capacity is $E_C^{(UE,l)}(\phi) l \omega_l E_C^{(UE,1)}(l \omega_l \phi)$, where $l \omega_l$ denote as the reliable tile as $l \omega_l = l - \sum_{g=0}^{\min(l, (1-\eta\psi)\rho M)} g \frac{C_s^{l(1-\eta\psi)\rho M-l}}{C_s^{(1-\eta\psi)\rho M-g}}$ [20], where the M denote the original unused spectrum bands of MBS_i , the ρ denote the proportion of the occupied tile by MBS_i in the S_{MBS_i} , the η denote the probability of MBS_i still occupying this tile, the ψ denote the percentage of still occupied of tile and g denotes the number of unoccupied tiles.
3. The delay bound probability $\Pr\{Delay > t_{dwell}\} = e^{-\phi \delta t_{dwell}}$ which is the probability of the UE can be completely uploading through the FBS_j within the t_{dwell} .
4. If $\Pr\{Delay > t_{dwell}\} = e^{-\phi \delta t_{dwell}} > \varepsilon^{UE}$, then l is increased and repeatedly perform step 2 to reduce the value of the delay bound probability $\Pr\{Delay > t_{dwell}\}$, where ε^{UE} is the infraction probability of UE. Otherwise, $l_{required}^{UE}$ is obtained.

For instance, we initially allocate $l = 1$ tile for an UE. The ϕ is founded such that $E_B^{UE}(\phi) = E_C^{(UE,1)} = 5$, where $\phi = 0.05$. The delay bound violation probability is $\Pr\{Delay > 10\} = e^{-0.05 \times 5 \times 10} = 0.08$, if $0.08 < 0.09$, the number of tiles for the UE is 10, so $l_{required}^{UE} = 10$.

Third, the $t_{expected}$ is calculated as follows. Let $R_{average}$ denote as the average transmission rate of the UE provided by FBS_j . Let $PL_{average}$ denote the as the average path loss of the UE during passing the coverage of FBS_j . Let $D_{transmitted}$ denote as the data which is already transmitted by MBS_i . Let D_{total} denote as the total transmitted data of the UE. The is $RSSI_{dB}$ the received signal strength indicator. The procedure of calculating $t_{expected}$ is given below.

1. The average transmission rate $R_{average}$ of the UE is $R_{average} = l_{required}^{UE} \times \log_2(1 + RSSI_{dB})$ by the Shannon theory [26], where $R_{average}$ is obtained by calculating $l_{required}^{UE}$. The accurate value of $RSSI_{dB}$ considers the effect of the path loss model, $RSSI_{dB} = SNR_{FBS_j} - PL_{average}$ where the average path loss is $PL_{average} = \frac{1}{2R} \int_0^{2R} 38.46 + 20 \log_{10}(d_{U,F_j}) + 0.7 d_{2D} dd_{U,F_j}$, where the R is the radius of FBS_j , the d_{U,F_j} is the distance between UE and FBS_j and $0.7 d_{2D}$ is the penetration loss due to internal walls.
2. The remainder data $D_{remainder} = D_{total} - D_{transmitted}$, and MBS_i sends the information to FBS_j via the backhaul network. Consequently, the expected transmission time is $t_{expected} = \frac{D_{remainder}}{R_{average}}$.

For instance, the average transmission rate of FBS_1 is $360 \text{ kHz} = \log_2(1 + 7) = 1 \text{ Mbps}$, where $RSSI_{dB} = 20 - 12.9718 = 7 \text{ dB}$. The average expected transmission time is $t_{expected} = \frac{D_{remainder}}{1M} = \frac{10M}{1M} = 10s$, where the user remainder data as $D_{remainder} = 15M - 5M = 10M$.

4.3. Phase III: Green handover decision

This phase finally makes a green handover decision as follows. The procedure of the green handover decision is given below.

1. If $l_{available}^{FBS_j} \geq l_{required}^{UE}$ and $t_{dwell} \geq t_{expected}$, then the IDLE FBS_j is woken up and enters the ACTIVE mode to perform the handover procedure of the inbound mobility from MBS_i to ACTIVE FBS_j .
2. If $l_{available}^{FBS_j} \geq l_{required}^{UE}$ and $t_{dwell} < t_{expected}$, or if $l_{available}^{FBS_j} < l_{required}^{UE}$, then the UE still communicates with the CN through MBS_i .

Fig. 10 gives an example for the green handover decision. The FBS_1 computes the $l_{required}^{UE}$ and $l_{available}^{FBS_1}$. The FBS_1 operates in the IDLE mode if $t_{dwell} < t_{expected}$. Then, the FBS_2 computes the $l_{required}^{UE}$ and $l_{available}^{FBS_2}$. If $l_{available}^{FBS_2} \geq l_{required}^{UE}$ and $t_{dwell} \geq t_{expected}$, then FBS_2 switches from IDLE mode to ACTIVE mode. The UE hands over from MBS_1 to FBS_2 . Finally, the detailed flow charts of the handover procedure [27], including the handover preparation, execution, and completion, are given in Fig. 11.

5. Performance analysis

In this section, a simple analytic model is developed to mainly analyze the average energy consumption of data transmission of UE for inbound mobility by the proposed scheme. We begin by defining a few symbols. The definition of notations is given in Table 3.

- P_{nj} : The probability of a handover which has not occurred from MBS_i to FBS_j .
- P_{cj} : The probability of the remaining data of UE which cannot be completely uploaded through FBS_j .
- E_{active} : The energy consumption of the ACTIVE FBS_j and an UE.

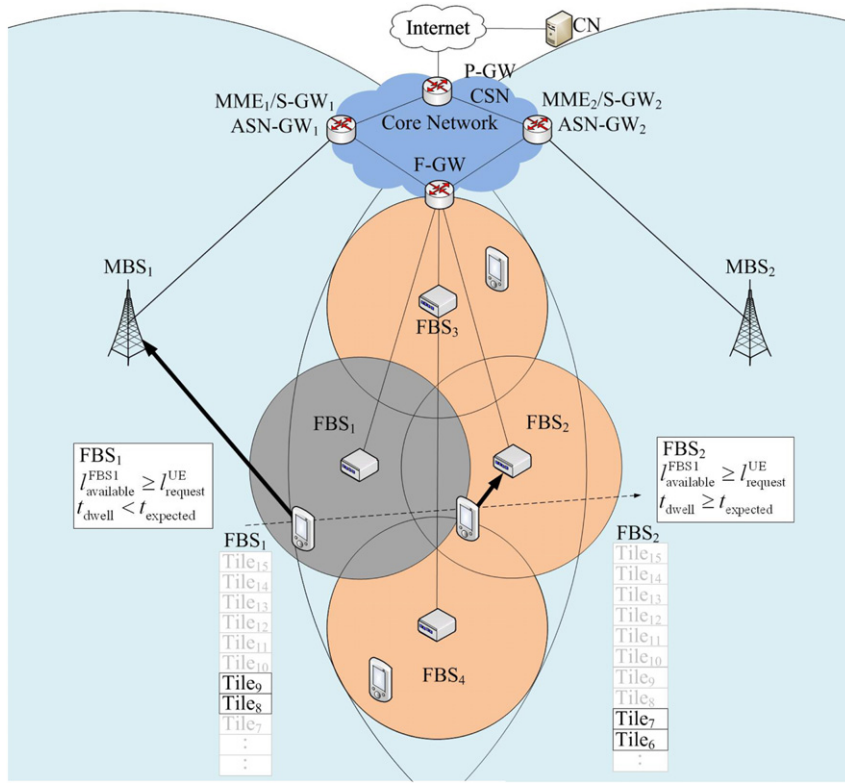


Fig. 10. The green handover decision.

Table 3

Definition of notation.

MBS_i	The i -th macro base station
FBS_j	The j -th femto base station
FBS_j^i	The neighboring FBSs of j -th FBS
t_{dwell}	User dwell time in the coverage of FBS_j
t_{expected}	Average expected transmission time of UE
S_{MBS_i}	The set of the original unused spectrum bands of MBS_i
SB_{MBS_i}	The set of occupied sub-bands by MBS_i
$SB_{FBS_j^i}$	The set of occupied sub-band by FBS_j^i
S_{occupied}	Total occupied spectrum band
$I_{FBS_j}^{\text{available}}$	Available bandwidth of FBS_j
t_{tp}	Total passing time of UE
$I_{\text{required}}^{\text{UE}}$	Required bandwidth of UE
R_{average}	Average transmission rate
α	The average variation of SNR at Δt
SNR_{MAX}	Maximum transmission power is received by FBS_j
ε^{UE}	Infraction probability of UE
$E_B^{\text{UE}}(\phi)$	Effective bandwidth of UE
$E_C^{(\text{UE}, 1)}(\phi)$	Effective capacity of the UE which is allocated by l tiles
$RSSI_{\text{dB}}$	Received signal strength indicator
PL_{average}	Average path loss of UE in the coverage of FBS_j
D_{total}	Total data of UE
$D_{\text{transmitted}}$	Data transmitted by MBS_i
$D_{\text{remainder}}$	Remainder data of UE

- E_{idle} : The energy consumption of the IDLE FBS_j and an UE.
- E_A : The average energy consumption for the data transmission of a UE using the Ashraf protocol.
- E_G : The average energy consumption for the data transmission of a UE using our proposed green handover protocol.

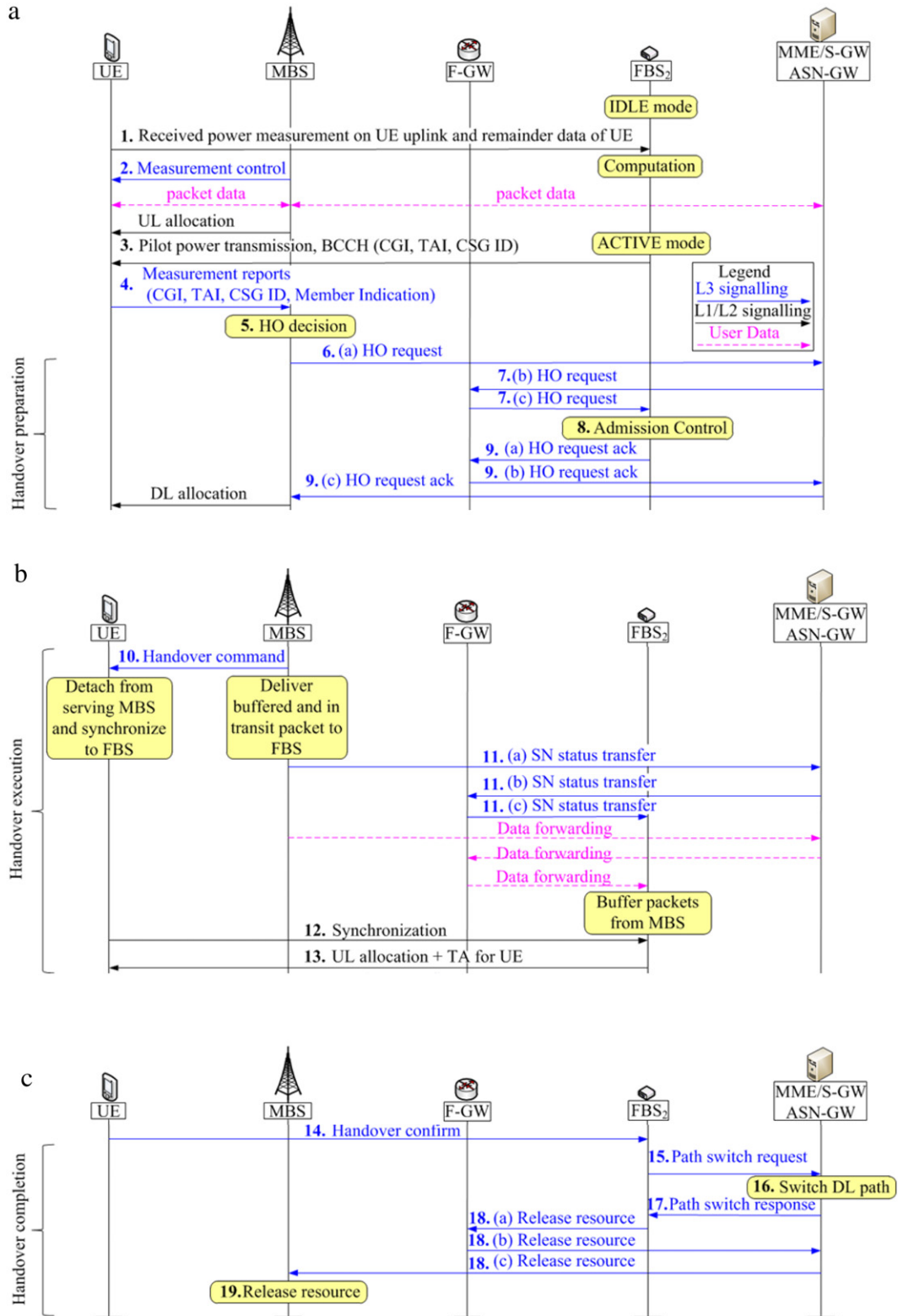


Fig. 11. The handover signaling flow of the proposed handover protocol. (a) Handover preparation. (b) Handover execution. (c) Handover completion.

The average energy consumption of the data transmission of an UE during an inbound mobility of the Ashraf protocol [17,18] is initially derived as follows.

Lemma 1. The average energy consumption for the data transmission of a UE performing the inbound mobility of existing protocol [17,18] is

$$E_A = E + \frac{1}{n} \sum_{j=1}^n (e^{-\lambda_j T_j} \times E_{\text{idle}} + (1 - e^{-\lambda_j T_j} \times E_{\text{active}})). \quad (1)$$

Proof. In general, the Poisson distribution is represented as $P(k, T) = \frac{(\lambda T)^k}{k!} e^{-\lambda T}$, where the k is the event number (the handover number in the analysis), T is the period time, and λ is the average proportion of the event happened. In this work, the $P(k, T)$ denotes the probability of k handover events occurring within the period time T . The Poisson distribution is to observe the probability of the handover number occurring within a period of time T . We assume that $P(k, T_j) = P(0, T_j)$ is equal to $P_{n_j} = e^{-\lambda_j T_j}$ to represent as the probability of a handover which has not occurred within time T_j , where $k = 0$. The probability of an inbound mobility not occurring from MBS_i to FBS_j is $P(k, T_j) = P(0, T_j) = P_{n_j} = e^{-\lambda_j T_j}$ under the Poisson distribution model, where $\lambda_j = \frac{1}{t_j}$ and t_j is the time period of the received SNR of FBS_j from the UE is larger than the threshold value. The $\lambda_j T_j$ is the average handover number within the time duration T_j , where T_j is equal to t_{tp} . The probability of handover is $1 - P_{n_j} = 1 - e^{-\lambda_j T_j}$. The average energy consumption $E_A = E + \frac{1}{n} \sum_{j=1}^n (e^{-\lambda_j T_j} \times E_{\text{idle}} + (1 - e^{-\lambda_j T_j}) \times E_{\text{active}})$ where E is the average energy consumption of the data transmission of an UE before entering the coverage of FBS_j . \square

For example, E is 0.2 W, E_{idle} is 6.2 W, and E_{active} is 10.2 W from Table 2, so $E_A = 0.2 + \frac{1}{1} \sum_{j=1}^1 e^{-0.5 \times 10} \times 6.2 + (1 - e^{-0.5 \times 10}) \times 10.2 = 10.37$ W.

Lemma 2. The average energy consumption of the data transmission of an UE performing the inbound mobility of our proposed protocol is

$$E_G = E + \frac{1}{n} \sum_{j=1}^n (e^{-\lambda_j T_j} \times E_{\text{idle}} + (1 - e^{-\lambda_j T_j}) \times (e^{-\hat{\lambda}_j t_{\text{dwell}_j}} \times E_{\text{idle}} + (1 - e^{-\hat{\lambda}_j t_{\text{dwell}_j}}) \times E_{\text{active}})). \quad (2)$$

Proof. The probability of a handover which has not occurred within time T_j is $P_{n_j} = e^{-\lambda_j T_j}$ which is the same as Lemma 1, but the probability, $1 - P_{n_j} = 1 - e^{-\lambda_j T_j}$, of a handover within time T_j is further divided into two probabilities; the probabilities of the remainder data can and cannot be completely uploaded through the FBS_j . The probability of the remainder data of UE cannot be completely uploaded within time t_{dwell_j} through the FBS_j is $P_{c_j}(0, t_{\text{dwell}_j}) = P_{c_j} = e^{-(\hat{\lambda}_j t_{\text{dwell}_j})}$, where the $\hat{\lambda}_j = \frac{1}{t_{\text{expected}_j}}$ is the average number of complete uploading within time t_{expected_j} , where t_{expected_j} is the average expected transmission time using FBS_j and t_{dwell_j} is the time starting from the UE communicating with FBS_j and stopping to communicate with FBS_j . Let the probability of the remainder data of UE can be completely uploaded through the FBS_j be $P_{c_j} = 1 - e^{-(\hat{\lambda}_j t_{\text{dwell}_j})}$. The probabilities of the remaining data that can and cannot be completely uploaded through the FBS_j are $e^{-\hat{\lambda}_j t_{\text{dwell}_j}}$ and $1 - e^{-\hat{\lambda}_j t_{\text{dwell}_j}}$, respectively. The energy consumption of probability of the handover occurring if using our scheme is $(1 - e^{-\lambda_j T_j}) \times (e^{-\hat{\lambda}_j t_{\text{dwell}_j}} \times E_{\text{idle}} + (1 - e^{-\hat{\lambda}_j t_{\text{dwell}_j}}) \times E_{\text{active}})$. Therefore, the average energy consumption of the data transmission of a UE during an inbound mobility of our proposed protocol is $E_G = E + \frac{1}{n} \sum_{j=1}^n (e^{-\lambda_j T_j} \times E_{\text{idle}} + (1 - e^{-\lambda_j T_j}) \times (e^{-\hat{\lambda}_j t_{\text{dwell}_j}} \times E_{\text{idle}} + (1 - e^{-\hat{\lambda}_j t_{\text{dwell}_j}}) \times E_{\text{active}}))$. \square

For example, E is 0.2 W, E_{idle} is 6.2 W, and E_{active} is 10.2 W from Table 2, $E_G = 0.2 + \frac{1}{1} \sum_{j=1}^1 e^{-0.5 \times 10} \times 6.2 + (1 - e^{-0.5 \times 10}) \times (e^{-0.1 \times 12} \times 6.2 + (1 - e^{-0.1 \times 12}) \times 10.2) = 9.18$ W.

Theorem 1. Based on the results of Lemmas 1 and 2, the average energy consumption of our proposed protocol is smaller than that of existing protocol [17,18], $E_G < E_A$, i.e.,

$$\begin{aligned} & E + \frac{1}{n} \sum_{j=1}^n (e^{-\lambda_j T_j} \times E_{\text{idle}} + (1 - e^{-\lambda_j T_j}) \times (e^{-\hat{\lambda}_j t_{\text{dwell}_j}} \times E_{\text{idle}} + (1 - e^{-\hat{\lambda}_j t_{\text{dwell}_j}}) \times E_{\text{active}})) \\ & < E + \frac{1}{n} \sum_{j=1}^n (e^{-\lambda_j T_j} \times E_{\text{idle}} + (1 - e^{-\lambda_j T_j}) \times E_{\text{active}}). \end{aligned} \quad (3)$$

Proof. Based on Lemma 1, the average energy consumption of the existing protocol [17,18] is $E_A = E + \frac{1}{n} \sum_{j=1}^n (e^{-\lambda_j T_j} \times E_{\text{idle}} + (1 - e^{-\lambda_j T_j}) \times E_{\text{active}})$. Based on Lemma 2, the average energy consumption of our proposed protocol is $E_G = E + \frac{1}{n} \sum_{j=1}^n (e^{-\lambda_j T_j} \times E_{\text{idle}} + (1 - e^{-\lambda_j T_j}) \times (e^{-\hat{\lambda}_j t_{\text{dwell}_j}} \times E_{\text{idle}} + (1 - e^{-\hat{\lambda}_j t_{\text{dwell}_j}}) \times E_{\text{active}}))$. It is easily seen that $E + \frac{1}{n} \sum_{j=1}^n (e^{-\lambda_j T_j} \times E_{\text{idle}} + (1 - e^{-\lambda_j T_j}) \times (e^{-\hat{\lambda}_j t_{\text{dwell}_j}} \times E_{\text{idle}} + (1 - e^{-\hat{\lambda}_j t_{\text{dwell}_j}}) \times E_{\text{active}})) < E + \frac{1}{n} \sum_{j=1}^n (e^{-\lambda_j T_j} \times E_{\text{idle}} + (1 - e^{-\lambda_j T_j}) \times E_{\text{active}})$. \square

Table 4
Simulation parameters.

Parameter	Value
Networks size	1000 m × 1000 m
MBS transmission range	1000 m
FBS transmission range	50 m
Velocity of UE	30–80 km/h
Number of FBSs	6
Data size	10–15 MB
Packet rate	1000 packets/s
Packet size	1000 bytes
Simulation time	20–40 s

Consequently, the average energy consumption of our proposed protocol is smaller than that of the Ashraf protocol [17,18], since $E_G = 9.18 \text{ W} < E_A = 10.37 \text{ W}$.

6. Simulation results

Our paper presents a green handover protocol in two-tier OFDMA macrocell–femtocell networks. To evaluate our green handover protocol, Ashraf et al.'s IDLE mode protocol [17], all these protocols are mainly implemented using the Network Simulator-2 (NS2) [28] and 3GPP module [29]. The system parameters are given in Table 4. To discuss the effect of simulation results, our simulation considers the networks size of 1000 m² and six FBSs are deployed in the overlapped area between the serving and next MBSSs. The communication radius of the FBS and the MBS are assumed to be 50 m and 1000 m, respectively. The data size changes from 10 to 15 MB and the velocity of a user changes from 30 to 80 km/h. The power consumption of the ACTIVE FBS assumes to be 10.2 W and the IDLE FBS assumes to be 6 W. The power consumption of LTE UE is mainly based on Table 2. The simulation scenario is that a UE is moving from the left to right. In this situation, the UE is passing six FBSs. It noted that some of them are IDLE FBS. When the UE is passing the coverage of the IDLE FBS, the IDLE FBS makes a decision to wake up to perform the handover procedure, or not to wake up and not to perform the handover procedure. The performance metrics to be observed are:

- *Power consumption (PC)*: The total power consumption of all MBS, FBSs and the UE.
- *Handover latency (HL)*: The time period between a UE changing its association from the current association MBS/FBS to another one.
- *Packet loss ratio (PLR)*: The total number of lost packets divided by the total number of transmitted packets during the handover period for a UE
- *Signaling cost of handover (SC)*: The total number of signal packets, including request packets and the responses packets communicating between MBS with FBS.

It is worth mentioning that a green handover protocol is achieved with low PC, low HL, low PLR, and low SC. In the following, we illustrate our simulation results for power consumption (PC), handover latency (HL), packet loss ratio (PLR), and signaling cost of handover (SC) from several aspects.

6.1. Power consumption (PC)

To illustrate the influence of the PC, Fig. 12(a) shows the simulation result of PC under the various data size (ranging from 10 to 15 MB). The simulated result illustrates that our green handover protocol significantly achieves energy saving. This is because that our protocol offers the non-frequently occurrence of the handover event to try to keeping the FBS at the IDLE mode. In general, the PC drops as the data size increases as illustrated in Fig. 12(a). It indicates that more power saving results will be achieved. This power-saving result also shows that the Ashraf protocol [17,18] has more handover events than our protocol. The power consumption of the Ashraf protocol is fixed at 42 W. The power consumption of our green handover protocol is less than 42 W. Fig. 12(b) illustrates the simulation result of PC vs. the velocity (ranging from 30 to 80 km/h). The power consumption of our green handover protocol is lower than that of the Ashraf protocol [17,18]. It is observed that the PC drops as the velocity increases. For instance, the power consumption is about 46 W if the velocity is 30 km/h, and the power consumption is about 41.28 W if the velocity is 80 km/h. This shows that the IDLE FBS has the high probability of keeping the FBS IDLE under the high speed environment.

6.2. Handover latency (HL)

Fig. 13 gives the simulation results of the average handover latency (HL). The lower the number of handovers is, the lower the average handover latency will be. Fig. 13(a) shows the HL vs. the data size (ranging from 10 to 15 MB). In general, the HL drops as the data size increases. For instance, the HL is 325 ms if the data size is 10 MB, and the HL is 74 ms if the data size is 15 MB of our green handover protocol, while the HL of the Ashraf protocol [17,18] is fixed at 360 ms. This is because a less frequent number of handover events occurs. Fig. 13(b) provides the simulation result of the average handover latency (HL) vs. the velocity of the UE (ranging from 30 to 80 km/h). We observed that the HL drops as the velocity increases. For

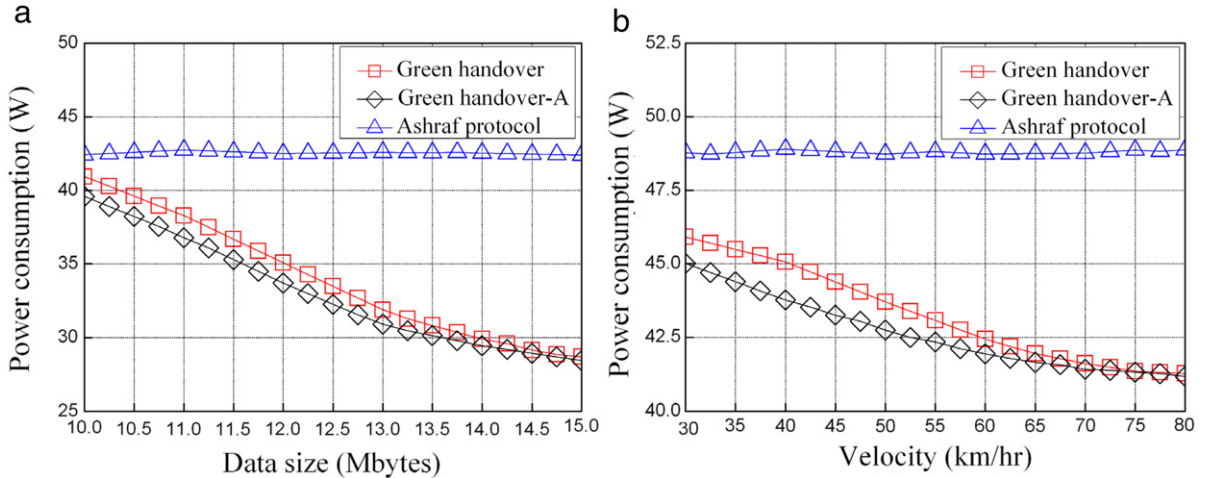


Fig. 12. (a) Power consumption vs. data size. (b) Power consumption vs. velocity.

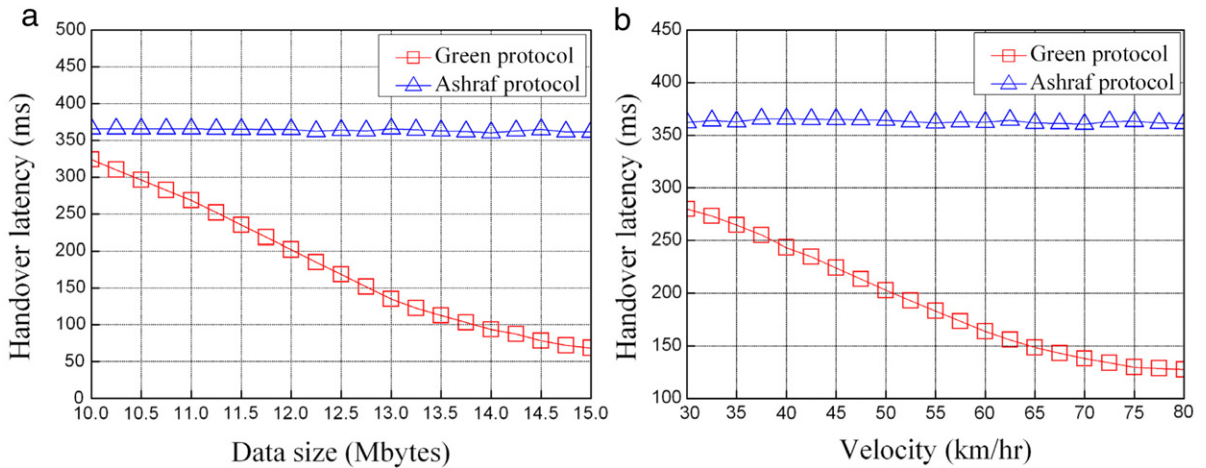


Fig. 13. (a) Handover latency vs. data size. (b) Handover latency vs. velocity.

instance, the HL is 275 ms if the the velocity is 30 km/h and the HL is 125 ms if the velocity is 80 km/h of our green handover protocol, while the Ashraf protocol [17,18] is fixed at 360 ms. According to the simulation result, the HL of the proposed protocol is better than the Ashraf protocol [17,18].

6.3. Packet loss ratio (PLR)

The simulation results of the packet loss ratio (PLR) under various data size and velocity are illustrated in Fig. 14. Fig. 14(a) shows the simulation result of PLR vs. the data size (ranging from 10 to 15 MB). The packet loss occurs when the handover is executed. In general, the PLR increases as the data size increases. For instance, the PLR of our protocol and Ashraf protocol is about 7% if the data size is 10 MB. The PLRs of our protocol and the Ashraf protocol are 11.67%, and 11.5% and 13.4% if the data size is 15 MB. The PLR of our protocol is smaller than that of the Ashraf protocol under various data size implying that the packet loss ratio is less than that of the Ashraf protocol. Fig. 14(b) shows the simulation result of the PLR vs. the velocity of the UE (ranging from 30 to 80 km/h). In general, the PLR increases as the velocity increases. The PLR of our protocol is smaller than that of the Ashraf protocol under the various velocity implying that the packet loss ratio is less than that of the Ashraf protocol. For instance, the PLR is 29% if the velocity is 80 km/h of our green handover protocol, and the PLR is 33% if the velocity is 80 km/h using the Ashraf protocol. Consequently, the packet loss ratio of the green handover protocol is smaller than that of the Ashraf protocol.

6.4. Signaling cost of handover (SCH)

Fig. 15 shows the simulation results of the signaling cost of handover (SCH). The higher the number of handovers is, the larger the SCH will be. Fig. 15(a) shows the simulation result of the SCH vs. the data size (ranging from 10 to 15 MB).

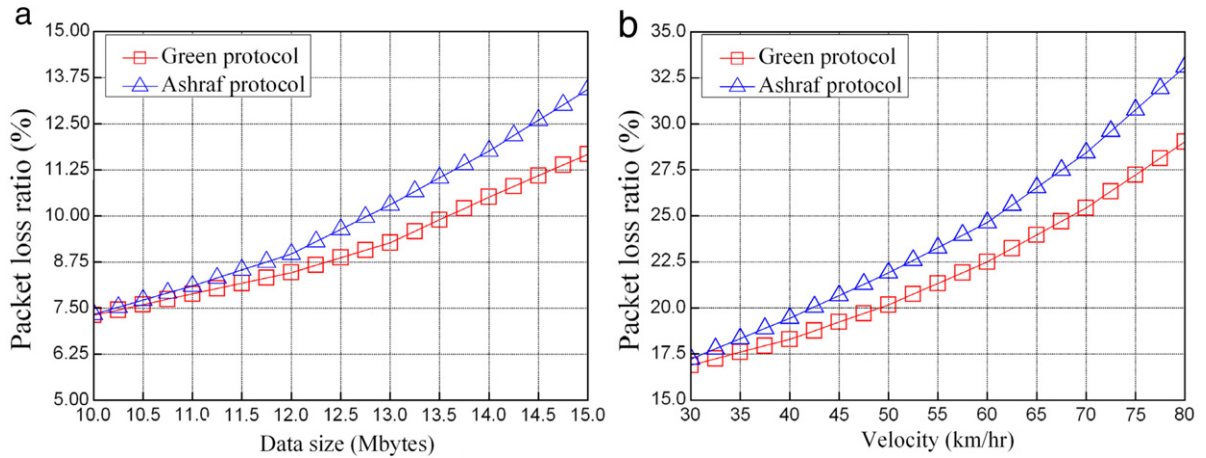


Fig. 14. (a) Packet loss ratio vs. data size. (b) Packet loss ratio vs. velocity.

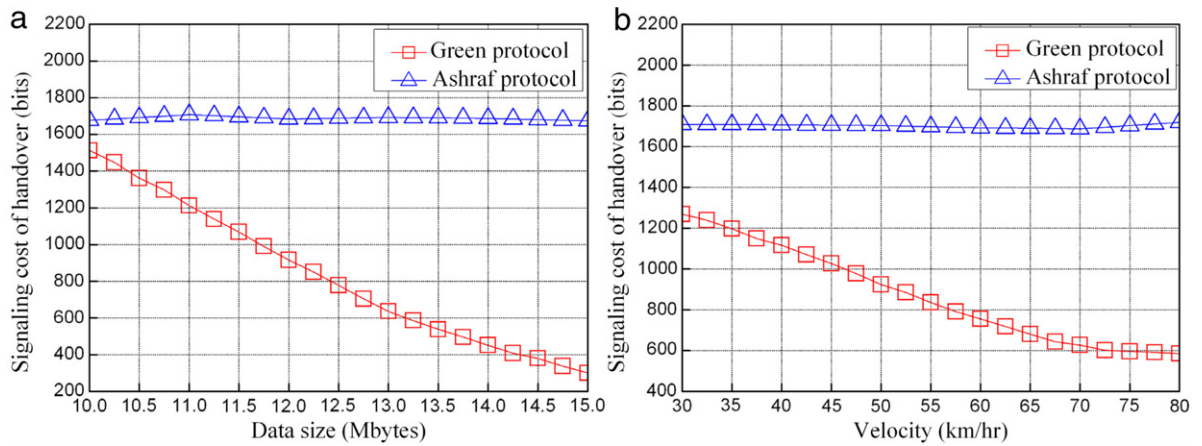


Fig. 15. (a) Signaling cost of handover vs. data size. (b) Signaling cost of handover vs. velocity.

The SCH indicates the number of information exchanges between UE and FBS. The SCH of our proposed scheme is smaller than the Ashraf scheme because of our proposed protocol efficiently reduces the undesired handover events. In general, the SCH decreases as the data size increases. For instance, the SCH is 1512 bits if the data size is 10 MB and the SCH is 300 bits if the data size is 15 MB. The SCH of the proposed protocol is smaller than that of Ashraf protocol under various data size. Fig. 15(b) offers the simulation result of the SCH vs. the velocity of the UE (ranging from 30 to 80 km/h). In general, the SCH decreases as the velocity increases, because that the number of handover events decreases. The SCH of the proposed protocol is smaller than that of the Ashraf protocol under various velocities. For instance, the SCH is fixed at 1700 bits under various velocities using the Ashraf protocol. In addition, the SCH of our protocol is extremely lower than that of the Ashraf protocol at 80 km/h.

7. Conclusions

In this paper, we have developed a green handover protocol in two-tier OFDMA macrocell–femtocell networks. A green scheme allows the femtocell base station to completely switch off its radio communication and associated processing when not involved in an active call. To improve the energy efficiency of the femtocell base station, the proposed green handover protocol can intelligently switch on its radio communication and associated processing to wake it up from the idle mode, if the remainder data of a mobile host can be completely uploaded through the wake-up femtocell base station. We have provided the mathematical analysis and the performance simulation to illustrate that the proposed protocol can significantly offer a more power-saving result compared with the existing energy-saving handover protocols.

Acknowledgments

This research was supported by the National Science Council of the ROC under Grant NSC-100-2219-E-305-001.

References

- [1] G.P. Fettweis, E. Zimmermann, ICT energy consumption — trends and challenges, in: Proc. of the International Symposium on Wireless Personal Multimedia Communications, Lapland, Finland, Sep 2008.
- [2] Femto Forum. <http://femtoforum.org/fem2/>, 2010.
- [3] C. Ball, T. Hindelang, I. Kambourov, S. Eder, Spectral efficiency assessment and radio performance comparison between LTE and WiMAX, in: Proc. IEEE International Symposium on Personal, Indoor and Mobile Radio Communications, PIMRC 2008, French Riviera, France, Sep. 2008, pp. 1–6.
- [4] Mobility support in IPv6, RFC 6275, July 2011. <http://www.hjp.at/doc/rfc/rfc3775.html>.
- [5] Proxy Mobile IPv6, RFC 5213, August 2008. <https://merlot.tools.ietf.org/html/rfc5213>.
- [6] Jong-Hyoun Lee, Youn-Hee Han, Sri Gundavelli, Tai-Myoung Chung, A comparative performance analysis on Hierarchical mobile IPv6 and proxy mobile IPv6, Telecommunication Systems 41 (4) (2009) 279–292.
- [7] Jong-Hyoun Lee, Thierry Ernst, Tai-Myoung Chung, Cost analysis of IP mobility management protocols for consumer mobile devices, IEEE Transactions on Consumer Electronics 56 (2) (2010) 1010–1017.
- [8] A. Golaup, M. Mustapha, L.B. Patanapongpibul, Femtocell access control strategy in UMTS and LTE, in: Proc. IEEE Communications Magazine, pp. 117–123.
- [9] Y. Shi, A.B. MacKenzie, L.A. DaSilva, On resource reuse for cellular networks with Femto- and Macrocell coexistence, in: Proc. IEEE Global Telecommunications Conference, Globecom 2010, Miami, American, Dec. 2010, pp. 1–6.
- [10] H. Zhou, H. Luo, H. Zhang, C.H. Lo, H.C. Chao, A Network-based global mobility management architecture, International Journal of Ad Hoc and Ubiquitous Computing 5 (1) (2010) 1–6.
- [11] A. Kumar, A.K. Sarje, M. Misra, Prioritised predicted region based cache replacement policy for location dependent data in mobile environment, International Journal of Ad Hoc and Ubiquitous Computing 5 (1) (2010) 55–67.
- [12] H. Oh, K. Yoo, J. Na, C. Kim, A seamless handover scheme in IPv6-based mobile networks, International Journal of Ad Hoc and Ubiquitous Computing 4 (1) (2010) 54–60.
- [13] J.M. Moon, D.H. Cho, Novel handoff decision algorithm in hierarchical Macro/Femto-cell networks, in: Proc. IEEE Wireless Communications and Networking Conference, WCNC 2010, Sydney, Australia, 2010, pp. 1–6.
- [14] S. Wu, X. Zhang, R. Zheng, Z. Yin, Y. Fang, D. Yang, Handover study concerning mobility in the two-hierarchy network, in: Proc. IEEE Vehicular Technology Conference, VTC 2009-Spring, Barcelona, Spain, 2009, pp. 1–5.
- [15] A. Ulvan, R. Bestak, M. Ulvan, The study of handover procedure in LTE-based femtocell network, in: Proc. IEEE Wireless and Mobile Networking Conference, WMNC 2010, Budapest, Hungary, Oct. 2010, pp. 1–6.
- [16] H. Zhang, X. Wen, B. Wang, W. Zheng, Y. Sun, A novel handover mechanism between femtocell and macrocell for LTE based networks, in: Proc. International Conference on Communication Software and Networks, ICCSN 2010, Singapore, Feb. 2010, pp. 228–231.
- [17] I. Ashraf, Lester T.W. Ho, H. Claussen, Improving energy efficiency of femtocell base stations via user activity detection, in: Proc. IEEE Wireless Communications and Networking Conference, WCNC 2010, Sydney, Australia, April. 2010, pp. 1–5.
- [18] H. Claussen, I. Ashraf, Lester T.W. Ho, Dynamic idle mode procedures for femtocells, Bell Labs Technical Journal 15 (2) (2010) 95–116.
- [19] 3GPP TS 36.927 V2.0.0, Potential solutions for energy saving for E-UTRAN (Release 10), May 2011.
- [20] S.Y. Lien, C.C. Tseng, K.C. Chen, C.W. Su, Cognitive radio resource management for QoS guarantees in autonomous femtocell networks, in: Proc. IEEE International Conference on Communications, ICC 2010, Cape Town, South Africa, May. 2010, pp. 1–6.
- [21] C.H. Ko, H.Y. Wei, On-demand resource-sharing mechanism design in two-tier OFDMA femtocell networks, IEEE Transactions on Vehicular Technology 60 (3) (2011) 1059–1071.
- [22] G. Cao, D. Yang, R. An, X. Ye, R. Zheng, X. Zhang, An adaptive sub-band allocation scheme for dense femtocell environment, in: Proc. IEEE Wireless Communications and Networking Conference, WCNC 2011, Quintana-roo, Mexico, March. 2011, pp. 102–107.
- [23] S. Wang, J. Wang, J. Xu, Y. Teng, K. Horneman, Cooperative component carrier (re-)selection for LTE-advanced femtocells, in: Proc. IEEE Wireless Communications and Networking Conference, WCNC 2011, Quintana-roo, Mexico, March. 2011, pp. 1–6.
- [24] 3GPP TR 36.814 V9.0.0, Evolved Universal Terrestrial Radio Access (E-UTRA); Further advancements for E-UTRA physical layer aspects (Release 9), March 2010.
- [25] P. Mohana Shankar, Fading and Shadowing in Wireless Systems, Springer, ISBN: 978-1-4614-0366-1, 2012.
- [26] C.E. Shannon, A mathematical theory of communication, Bell System Technical Journal 27 (1948) 379–423. 623–656.
- [27] 3GPP TS 36.300 V10.3.0, Evolved Universal Terrestrial Radio Access (E-UTRA) and Evolved Universal Terrestrial Radio Access Network (E-UTRAN); Overall description; Stage 2 (Release 10), April 2011.
- [28] The Network Simulator NS-2. <http://stuweb.ee.mtu.edu/ljalian/>.
- [29] Enhanced UMTS Radio Access Network Extensions for NS-2 (EURANE). <http://eurane.tiwmc.nl/eurane/>.